JOURNAL OF CATALYSIS **124,** 520–529 (1990)

Highly Dispersed Rh/SiO$_2$ and Rh/MnO/SiO$_2$ Catalysts

1. Synthesis, Characterization, and CO Hydrogenation Activity

K. P. DE JONG, J. H. E. GLEZER, H. P. C. E. KUIPERS,
A. KNOESTER, AND C. A. EMEIS

*Koninklijke/Shell-Laboratorium, Amsterdam, (Shell Research B. V.), Badhuisweg 3,
1031 CM Amsterdam, The Netherlands*

Received April 11, 1989; revised December 11, 1989

Investigation has been made of the influence of a high Rh dispersion in silica-based Rh and Rh/MnO catalysts (i) on the direct conversion of synthesis gas and (ii) on the activity enhancement due to the presence of MnO which has been reported for catalysts displaying a medium Rh dispersion. Highly dispersed Rh/SiO$_2$ and Rh/MnO/SiO$_2$ catalysts (2–6 wt% Rh) were prepared by deposition–precipitation techniques. Hydrogen chemisorption showed the Rh dispersion to be very high for both the monometallic and the bimetallic catalysts (H/Rh $\geq$1 for all cases). Electron microscopy revealed a uniform distribution of the Rh particles (~1 nm) over the silica carrier. Since the hydrogen uptake capacities of Rh/SiO$_2$ and Rh/MnO/SiO$_2$ were fully on a par, it was concluded that probably no large amounts of MnO are present on the Rh surface in the bimetallic catalysts. Infrared spectra of adsorbed CO, however, provided evidence that the presence of MnO modifies the chemisorptive properties of metallic Rh. Comparison of the highly dispersed catalysts with catalysts of medium dispersion for the conversion of synthesis gas at elevated pressures revealed a shift toward methanol as the main product. Surprisingly the presence of MnO does not affect to a large extent the activity at high Rh dispersions, whereas at medium dispersion a five- to tenfold increase in the turnover frequency for CO hydrogenation was observed. The fact that the promoting effect of MnO is not operative with small Rh particles is attributed to the absence of MnO on the metal surface.

INTRODUCTION

Supported rhodium catalysts for the conversion of synthesis gas have received considerable attention since they are interesting from both a practical and a theoretical point of view. Rhodium is unique in exhibiting fairly high selectivities for the direct conversion of synthesis gas to two-carbon-containing oxygenates, especially ethanol (*1, 2*). Moreover, considerable effects of the carrier used (*3*), the presence of oxidic additives (MnO, MoO$_2$) (*2, 4*), and the metal dispersion (*5, 6*) have been described. Restricting ourselves to silica-supported catalysts, the metal dispersions deduced from hydrogen chemisorption (H/Rh) fall in the range H/Rh = 0.2–0.8 (*5, 6*). It has been observed that an optimum dispersion seems to exist for ethanol (H/Rh $\simeq$ 0.35) while the methanol selectivity steadily increases with H/Rh (*5*). The most extensive studies have been made with Rh/SiO$_2$ catalysts exhibiting a medium dispersion (4–5 nm Rh particles). With this type of catalyst, detailed mechanistic studies have been performed by van den Berg (*4*). Furthermore a five- to tenfold activity enhancement was observed to be brought about by the addition of MnO (and MoO$_2$) (*2, 4*).

We have addressed the following questions. Can even higher Rh dispersions (viz., H/Rh $\geq$1) be prepared on silica and what activity/selectivity phenomena will then be observed? Second, is the activity enhancement effect of MnO also apparent with extremely small Rh particles of ~1 nm? Until now no definite reports have been available

0021-9517/90 $3.00

in the literature for Rh/SiO_2 catalysts which display a hydrogen uptake $H/Rh > 1$. Catalysts prepared by conventional impregnation and drying techniques as well as those derived from organometallic precursors (*7*) or well-defined clusters (*8*) contain 4- to 5-nm Rh particles after a hydrogen treatment at temperatures at or above 200°C.

In this paper we describe the preparation of highly dispersed Rh/SiO_2 and $Rh/MnO/SiO_2$ catalysts by applying deposition–precipitation via urea decomposition. This synthesis route leads to uniform and often highly dispersed catalysts and has been extensively described by Geus and co-workers (*9*) for nonporous, powdered silica carriers. We have successfully applied this method while using a preformed silica and still working with the advantageous, diluted solutions. The catalysts thus prepared have been characterized in great detail concerning the metal dispersion and the location of Rh and MnO with respect to each other in the bimetallic catalysts. The characterization techniques applied were electron microscopy, hydrogen chemisorption, and infrared spectroscopy of adsorbed CO. The catalysts have been tested for the direct conversion of synthesis gas. Advanced characterization studies with these catalyst systems using X-ray photoelectron spectroscopy (*10*) and low energy ion scattering spectroscopy (*11*) will form Parts 2 and 3, respectively.

EXPERIMENTAL

Catalyst Preparation

Silica-supported catalysts were prepared by deposition–precipitation via urea decomposition. This method is based on the deposition of the hydroxide (or a basic salt) in question by slowly generating hydroxyl ions via the hydrolysis of urea. The rate of production of hydroxyl ions is kept low in order to prevent precipitation in the bulk of the liquid and to facilitate nucleation at the support surface. Details concerning the preparation performed are given below.

Rh/SiO_2, MnO/SiO_2, and $Rh/MnO/SiO_2$ catalysts were prepared as outlined above. The bimetallic $Rh/MnO/SiO_2$ catalysts were prepared in one step by simultaneous precipitation of the metal hydroxides. In a 500-ml double-walled, thermostatted, stirred vessel we dissolved the appropriate amount(s) of metal salt. We always used $RhCl_3 \cdot 3\,H_2O$ and/or $Mn(NO_3)_2 \cdot 4\,H_2O$ as starting compounds. After acidification with nitric acid ($pH \simeq 2$) we added 10 g of silica granules (Grace Davison silica gel,[1] PV = 1.2 ml g^{-1}, SA = 304 $m^2\,g^{-1}$, size of the granules 0.6–1.4 mm). Urea was added in excess (urea/metal ratio $\simeq 10$) at room temperature. With stirring, the mixture was heated to 90°C in a nitrogen atmosphere for about 18 h. At that temperature the following reactions take place:

$$(NH_2)_2CO + 3\,H_2O \rightarrow CO_2 + 2\,NH_4^+ + 2\,OH^-$$

$$M^{n+} + n\,OH^- \rightarrow M(OH)_n \downarrow$$

During the reaction, which leads to precipitation of the metal hydroxide(s) concerned, we measured the pH as a function of time. We also performed the precipitation without a carrier present. This enabled us to study the precipitation process in more detail. After the reaction the loaded support was separated from the liquid by filtration, washed extensively, and dried at 120°C. A survey of the catalysts is given in Table 1.

Catalyst Characterization

The elemental compositions of the dried catalysts were obtained by a combination of analytical techniques. The Rh content was determined by plasma emission spectroscopy, Mn by atomic absorption spectroscopy, and Cl by a coulometric method (*12*).

The dispersion of the metallic Rh particles in the catalysts was studied by H_2 chemisorption using a glass high-vacuum and volumetric gas-dosing system. Prior to the adsorption measurement the catalysts were

---

[1] Trace analysis revealed the presence of the following impurities: Al (600 ppm), Ba (40), Na (840), and Ti (200).

TABLE 1

Survey of Catalysts

Code	wt% Rh	wt% Mn	Cl/Rh atomic ratio
U02	2.1	—	0.026
U19	4.4	—	nd
U20	6.5	—	nd
U14	—	2.3	nd
U18	2.0	2.1	nd
U22	3.7	2.1	nd

Note. nd, not determined. The metal loadings and Cl contents were determined by elemental analysis after drying at 120°C (fresh).

reduced (25 vol% H_2 in Ar) and evacuated at elevated temperature (usually 400°C, ultimate pressure 10^{-6} Torr). At room temperature an adsorption isotherm was measured in the pressure range 0–12 Torr. By extrapolation to the zero-pressure axis we determined the monolayer uptake of the catalysts.

Transmission electron microscopy was carried out using a Philips EM401 microscope. Suitable samples of the catalysts were obtained by grinding, suspending the powder in butanol, and distributing the suspension on a carbon film.

TABLE 2

Hydrogen Uptake of Rh/SiO_2 Catalysts after Different Consecutive Reducing Pretreatments

Catalyst	wt% Rh	Reduction		H/Rh (at/at)
		No.	T(°C)	
U02	2.1	1	250	1.33
		2	400	1.20
U19	4.4	1	250	1.26
		2	400	1.04
U20	6.5	1	250	1.00
I48	2.3	1	250	0.06
		2	400	0.37

Note. Catalysts designated by "U" have been prepared by deposition–precipitation; catalyst I48 has been prepared by impregnation with $RhCl_3$ solution and drying.

TABLE 3

Hydrogen Uptake of $Rh/MnO/SiO_2$ Catalysts after Consecutive Reduction at Different Temperatures

Catalyst	wt% Rh	wt% Mn	Consecutive reduction		H/Rh atomic ratio
			No.	T(°C)	
U18	2.0	2.1	1	250	1.32
			2	400	1.09
			3	250	1.10
U22	3.7	2.1	1	250	1.30
			2	400	1.10

The surface condition of reduced catalysts was probed by studying infrared spectra of adsorbed CO. *In situ* FTIR spectra were recorded after pumping off the gaseous CO at ambient temperature and 200°C. All spectra were corrected for background absorption by the SiO_2 support.

Conversion of Synthesis Gas

The catalytic experiments were carried out in a stainless-steel, fixed-bed reactor lined with copper. Details concerning the reactor system and the on-line GLC system have been described elsewhere (*4*). In order to minimize temperature gradients during the highly exothermic reaction we always diluted the catalyst (2 ml) with silicon carbide (3 ml), as in previous work (*4*). Prior to the activity measurement the catalysts were reduced at 250°C in 10 vol% H_2 in He at 1 atm. Activity and selectivity data of the slowly deactivating catalysts were always reported after 8 h on stream.[2]

RESULTS

Catalyst Preparation

From pH measurements as well as visual inspection it appeared that the deposition of hydrolyzed Rh species onto the silica carrier takes place starting at pH 4. At pH 6 the

---

[2] The rate of deactivation was comparable to that reported in Ref. (*4*).

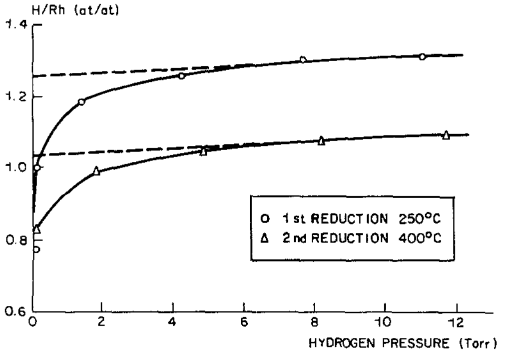

FIG. 1. Hydrogen adsorption isotherms for catalyst U19.

deposition of Rh was observed to be virtually complete. With manganese, on the other hand, the deposition takes mainly place at constant pH (pH 6). The precipitation of Rh and Mn in the synthesis of the bimetallic catalysts (U18 and U22, Table 1) seemed to occur sequentially. The pH curve for the bimetallic catalyst synthesis closely resembled the sum of the two curves for the monometallic systems, with deposition of Rh starting at pH 4 prior to that of Mn at pH 6.

Catalyst Characterization

Hydrogen chemisorption. Tables 2 and 3 summarize H/Rh values for several Rh/SiO_2 catalysts and $Rh/MnO/SiO_2$ catalysts, respectively. Typical adsorption isotherms have been reproduced in Fig. 1 (*2*), which show that even at pressures up to 10 Torr some increase in the H_2 uptake takes place. From the data obtained with catalyst U18 (Table 3) we can conclude that reduction and outgassing at 250°C suffice in obtaining a clean metal surface when one is working with precipitation catalysts. The results for

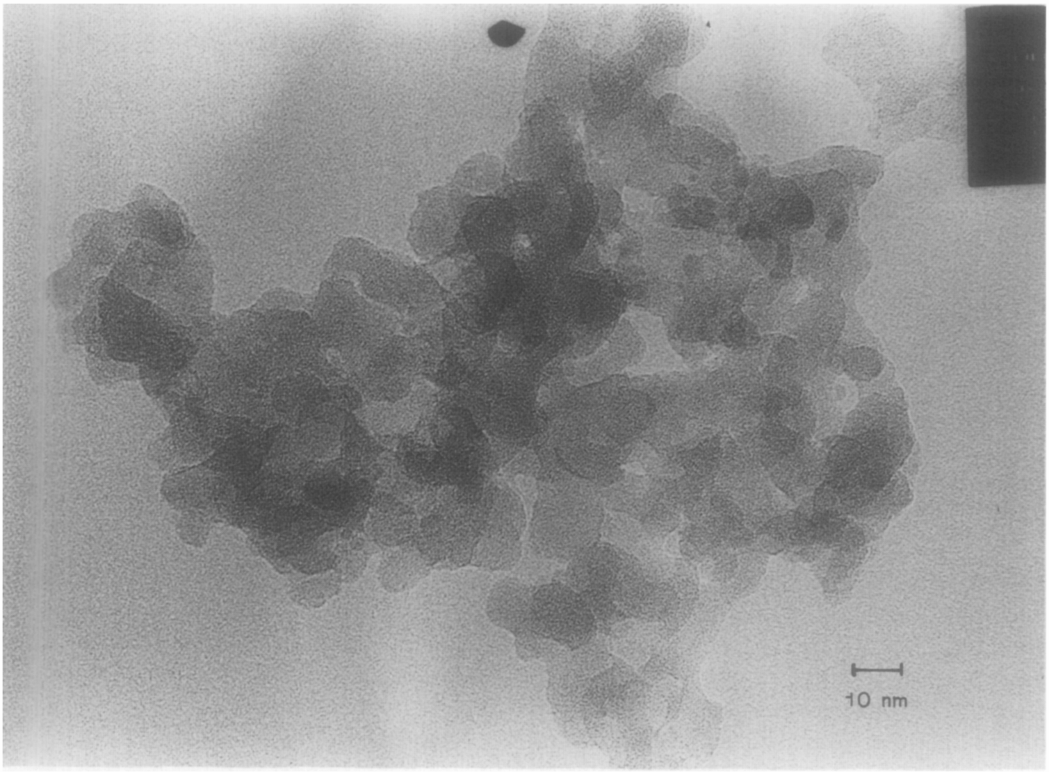

FIG. 2. TEM micrograph of MnO/SiO_2 catalyst U14. No discrete MnO phase can be detected on the ~10-nm silica particles.

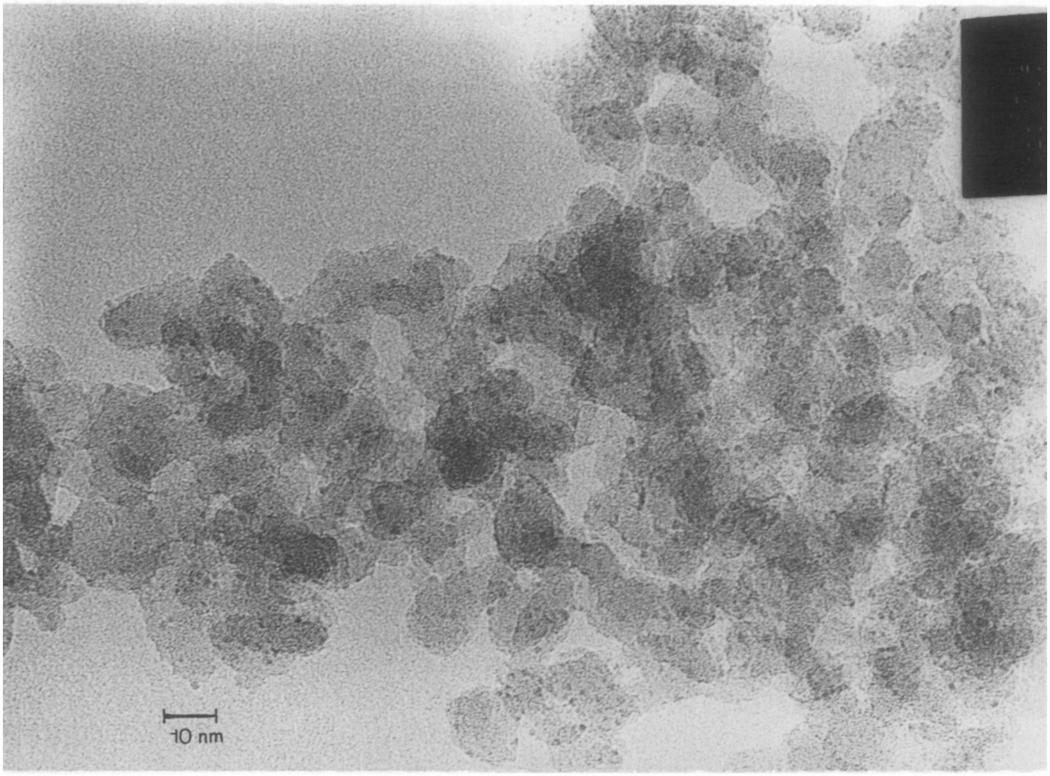

FIG. 3. TEM micrograph of Rh/SiO_2 catalyst U19 (containing 4.4 wt% Rh). This sample had been reduced at 250°C and exhibited a hydrogen uptake of H/Rh = 0.88.

catalyst I48, on the other hand, show that impregnation catalysts must be pretreated at 400°C in order to arrive at complete reduction (Table 2). We ascribe the low H_2 uptake of catalyst I48 after reduction at 250°C to residual chlorine which originates from the $RhCl_3$ used for the impregnation. The low chlorine content of the fresh precipitation catalysts (e.g., U02 in Table 1) leads to a facilitated reduction which is complete at 250°C.

From the H/Rh values for the precipitation catalysts we conclude that the Rh dispersion attained with silica as a support is very high. Assuming an upper limit of the adsorption stoichiometry of $H/Rh_s = 2$ (*13*), we calculate maximum values for the sizes of the metallic particles between 1.6 and 2.2 nm. Moreover, a high thermostability is inferred since $H/Rh \geq 1$ even after reduction at 400°C.

Most interestingly, the H_2 uptake capacities of Rh and Rh/MnO catalysts are completely comparable (cf. Tables 2 and 3). From these results it appears that MnO does not suppress the H_2 chemisorption, which makes it less likely that MnO covers up the Rh surface to a large extent. It should be noted that the reduction of MnO to Mn metal, which might interfere with H_2 adsorption on Rh, is highly unlikely, even when in contact with Rh. That the reduction is unlikely is based on thermodynamic arguments and experimental evidence from the literature on $Rh/MnO/SiO_2$ catalysts (*19*). In other words, manganese will not positively contribute to the H_2 uptake capacity of the bimetallic catalysts.

Transmission electron microscopy. Figure 2 is a representative micrograph of MnO/SiO_2 (U14), which shows the typical image of the silica carrier used. No discrete

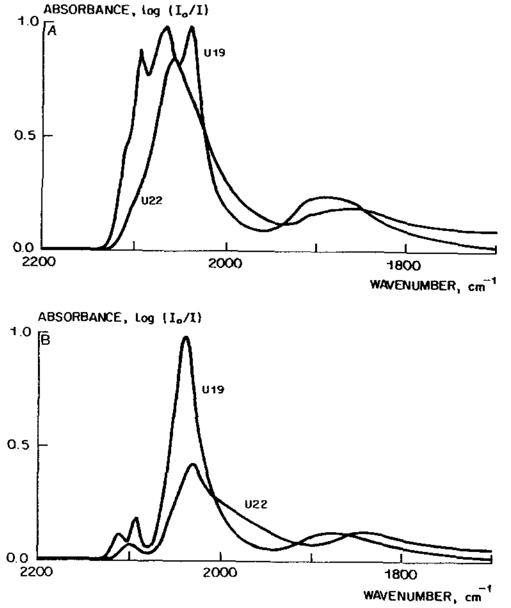

FIG. 4. Infrared absorption spectra of CO adsorbed on Rh/SiO$_2$ (U19) and Rh/MnO/SiO$_2$ (U22) after evacuation at ambient temperature (A) and at 200°C (B).

MnO particles or patches could be observed. We therefore conclude that MnO is present in a highly dispersed form on the support surface.

An extensive study of the monometallic Rh/SiO$_2$ catalysts was made. A very uniform distribution of the active component over the support was always observed while the particle size distribution was narrow. Concerning the reduced (250°C) catalyst U02 (2.1 wt% Rh), we established an upper limit of the Rh particles of 1.5 nm while the majority were smaller than 1 nm. Because of the very high Rh dispersion we think that a fraction of the particles even escaped detection. With catalyst U19 containing 4.4 wt% Rh we studied both a fresh and a reduced sample (reduction in 1 atm H_2 at 250°C, H/Rh = 0.88). A micrograph of the reduced catalyst is shown in Fig. 3, which clearly demonstrates the uniformity of the metal distribution. The dimensions of the metallic Rh particles in this case are in the range 0.5–1.7 nm. The average diameter is estimated to be 1.3 ± 0.3 nm. With the fresh catalyst U19 it was hard to detect discrete Rh oxide particles although a large number of particles smaller than 1 nm appeared to be present. These TEM results point to some minor sintering of Rh species during reduction. We think that a fresh catalyst contains both small clusters of Rh oxide and atomically dispersed Rh ions exchanged at the silica surface.

Infrared spectra of adsorbed CO. CO adsorbed on the reduced catalysts displays very intense absorption bands both for Rh/SiO$_2$ (U19) and for Rh/MnO/SiO$_2$ (U22). Figure 4A shows spectra obtained after pumping off CO at room temperature, and Fig. 4B after subsequent evacuation at 200°C. The assignment of the bands based on literature data (*14–17*) is given in Table 4.

After evacuation at room temperature the integrated band intensities for both catalysts are comparable. The most pro-

TABLE 4

Assignment of Infrared Absorption Bands of Adsorbed CO after Evacuation at Ambient Temperatures and at 200°C

Catalyst:	Rh/SiO$_2$ (U19)	Rh/MnO/SiO$_2$ (U22)
	Evacuation at ambient temperature	
Adsorption complex		
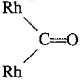	1800 (br)	1860 (br)
Rh—C≡O	2067 (s)	2058 (s)
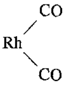	2040/2093	—
Rh^{3+} (?)	2108 (sh)	2100 (sh)
	Evacuation at 200°C	
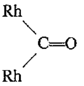	1872 (br)	1836 (br)
Rh—C≡O	2038 (s)	2030 (m)
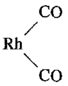	?/2092 (w)	?/2098 (w)
Rh^{3+} (?)	2110	—

Note. The bands are characterized by the wavenumber value at the band maximum (cm^{-1}) and their intensity (s, strong; w, weak, sh, shoulder; br, broad).

TABLE 5

Conversion of Synthesis Gas

Origin	This work		Ref. (*2*)	
Catalyst	Rh/SiO_2 (2.1/100)	$Rh/MnO/SiO_2$ (2.0/2.1/100)	Rh/SiO_2 (2.4/100)	$Rh/MnO/SiO_2$ (2.4/1.3/100)
H/Rh	1.33	1.32	~0.30	~0.30
TON × 10^2 (s^{-1})	0.6	1.1	3.0	32.
Selectivity (%C)				
CH_4	16	24	53	30
CH_3OH	47	36	—	—
C_2–oxygenates	25	27	43	58
C_2^+	5	6	4	12
C_3^+–oxygenates	7	6	—	—

Note. Reaction conditions in this work: 250°C, 95 bar, $CO/H_2 = 1/1$, GHSV = 5000 Nl · $liter^{-1} \cdot h^{-1}$. Reaction conditions in Ref. (*2*): 300°C, 70 bar, $CO/H_2 = 1/1$, GHSV = 25000 Nl · $liter^{-1} \cdot h^{-1}$.

nounced differences between the spectra in Fig. 4A are that for the bimetallic catalyst (i) the bands have shifted to lower frequencies (10–20 cm^{-1}) and (ii) the fine structure of the high-frequency band is no longer observed. It appears that for $Rh/MnO/SiO_2$ the intensity of linearly adsorbed CO has grown at the expense of the gem–dicarbonyl complex, $Rh(CO)_2$. Figure 4B shows, moreover, that the intensity decrease of the absorption bands upon evacuation at 200°C[3] is more pronounced for the bimetallic catalyst. This suggests that the number of sites that strongly bind CO has decreased in the presence of MnO. Under Discussion we will consider these observations in more detail.

Catalytic Performance

Conversion of synthesis gas. The activity and selectivity data obtained for two precipitation catalysts and two impregnation catalysts (data from Ref. (*2*) in the latter case) have been collected in Table 5. As has been described before, (*2, 4*) with the impregnation catalysts a six- to tenfold increase in the overall activity is caused by the presence of oxidic additives. The precipitation catalysts, on the other hand, are influenced by the presence of MnO to a much smaller extent only. In both cases, the presence of MnO does not appreciably affect the selectivity pattern. Highly dispersed Rh catalysts, however, display a shift toward methanol as far as product selectivity is concerned (Table 5).

DISCUSSION

Catalyst Preparation and Rh Dispersion

In this section we focus on the extremely high Rh dispersions which we have obtained even at high loading via deposition–precipitation (Table 2). At a metal loading of 2.3 wt% and reduction at temperatures between 250 and 400°C, all characterization techniques point to an average Rh particle size of around 1.0 nm. At higher loadings (6.5 wt%) the average particle size increases to 1.3 nm. We note that the high dispersions are independent of the type of silica used and have been reproduced with a high-purity silica (Aerosil 300) (*18*). These observations raise the intriguing question as to which factors determine these high disper-

---

[3] Carbon deposition due to CO decomposition appeared to be negligible under these conditions since the spectra of Fig. 4 could be restored by readsorption of CO at room temperature.

sions (which have not been reported before with a silica carrier) and the thermostability during hydrogen treatment.

Preparation via impregnation and drying techniques typically leads to dispersions of 0.3 (*19*) to 0.4 (*4*) when using $RhCl_3$ as a precursor, whereas using $Rh(NO_3)_3$ has led to dispersions below 0.1 (*20*). Two factors contribute to these low dispersions, viz., a low dispersion of the metal precursor and a high mobility of this precursor during thermal treatment. Nitrates are known for their volatility, thereby leading to considerable sintering (*21*), which explains the results of Niwa and Lunsford (*20*). We think that $RhCl_3$ is also rather mobile, which has a detrimental impact on the dispersion.

The effects of the metal precursor are apparent by considering preparation routes in which initially an atomic dispersion is realized. Decanio *et al.* (*7*) produced Rh/SiO_2 by reduction of a silica-bound diallylrhodium complex at 200°C for 2 h. A 1.4 wt% Rh/SiO_2 catalyst thus prepared contained particles in the range 4–5 nm, clearly larger than those in our work. Katzer *et al.* (*22*) prepared 0.89 wt% Rh/SiO_2 by an ion-exchange technique (not further described) which led to $H/Rh = 0.99$ after reduction at 200°C for 4 h.

Two factors determine, in our opinion, the resulting dispersion in these Rh/SiO_2 catalysts. First, the homogeneity of the metal distribution over the carrier particles is of relevance. In situations of "clustering" of metal precursor during preparation, the dispersion after mild reduction may be high but will rapidly drop after more severe pretreatments. The precipitation techniques applied by us ensure a good homogeneity of the metal distribution.

Second, from the results cited above we conclude that the interaction between the reduced Rh particles and the silica also plays a role in their stabilization. An enhanced metal–support interaction greatly facilitates preparation and stabilization of extremely small Rh particles. Using γ-Al_2O_3 as a carrier it is relatively easy to stabilize Rh particles of 1 nm or even smaller (*23*). The interaction with γ-Al_2O_3 has been explained by the occurrence of metal *ions* (*24*) or metal *atoms* trapped by oxygen vacancies (*23*). Furthermore, by modifying silica with either Sn or Pb ions Zaikovskii *et al.* (*25*) obtained 2-nm Rh particles after reduction at 600°C (!).

Summarizing, we note that the origin of the small Rh particles (≈1 nm), which have not been obtained before on a pure silica, lies in (i) a very high dispersion of the metal precursor, (ii) the absence of detrimental anions which facilitate migration, and (iii) possibly the stabilization of the metallic Rh particles by the support. Two types of metal–support interaction may underlie the stabilization. One possibility is the presence of Rh-ions in a silicate-type structure which anchor the Rh particles, as has been reported before, e.g., with Ni (*26*). An enhanced physical interaction (epitaxy) because of a (local) recrystallization of the silica surface during preparation is another possibility. Both types of interaction strongly depend on the preparation procedure and are promoted by the precipitation conditions (pH, temperature, time) applied in this work. We refer to a study on Cu/SiO_2 catalyst (*27*), which shows that synthesis parameters have a large impact on the genesis and structure of the metallic crystallites.

Interaction between Rh and MnO

In this section we concentrate on the *location* of Rh and MnO with respect to each other and the *nature* of the interaction for catalysts prepared by deposition–precipitation.

Both hydrogen chemisorption and spectroscopic techniques (*10, 11*) indicate that for the highly dispersed catalysts the metallic Rh surface is not covered up by MnO to a measurable extent. Most likely, Rh and MnO are randomly deposited on the support with respect to each other. Infrared spectra of adsorbed CO (cf. Fig. 4), however, show that MnO has an influence on the adsorptive properties of Rh. The presence of MnO suppresses the occurrence of gem–dicarbonyl species at the surface while the number of sites strongly bonding CO is reduced. Recently, van 't Blik *et al.* (*23*) presented evidence that CO adsorption on small Rh clusters, which gives rise to gem–dicarbonyl species, is accompanied by a breaking up of the metallic particles (Rh–Rh bonds were no more observed by EXAFS). This phenomenon is limited to very small Rh particles (*15, 23*). Apparently, in our samples the presence of MnO inhibits the CO-induced breaking up of Rh particles. One may ascribe this effect of MnO to enhanced interaction between metallic Rh and patches of (nonstoichiometric) manganese oxide whereby the surface structure of Rh will resemble those of larger crystallites, viz., flat planes (*28*). Similar phenomena have been reported for TiO_2-supported catalysts (*29*) and with Cu/SiO_2 (*27*).

An alternative explanation, which cannot be fully excluded as yet, is that a limited amount of MnO present at the Rh surface decreases the heat of adsorption of CO (as is indeed suggested by the spectra of Fig. 4B), thereby preventing the breaking up of the particles.

Influence of Rh Dispersion and MnO Addition on the Catalytic Properties

From the results summarized in Table 5 it appears that with increasing Rh dispersion the product pattern shifts from methane and C_2 oxygenates toward mainly methanol. This observation is fully in accordance with a paper of Arakawa *et al.* (*5*). From previous work (*6*) the mode of CO adsorption appears to shift from bridged to linear when going from low to high Rh dispersion. Therefore, we tentatively relate the high methanol selectivity at high Rh dispersion with the predominant occurrence of linearly adsorbed CO (cf. Fig. 4). Note that CO dissociation is not required for methanol production, and is anyway less probable for linearly adsorbed CO.

Addition of MnO to Rh/SiO_2 catalysts may lead to considerable activity enhancements by, say, a factor of 5 to 10. These promoting effects have been reported previously (*2, 4*) and are reproduced in Table 5. No significant selectivity changes have been observed. With these Rh catalysts, which display a medium dispersion, the effects of MnO have been ascribed to its presence at the Rh surface (*4, 19*), which may facilitate CO dissociation (*30*). The highly dispersed Rh catalysts considered in this work do not display such a large activity increase upon MnO addition (Table 5). The activity enhancement here is a factor of 2 at most. In view of the above results with larger Rh particles it might be concluded that MnO is not present at the Rh surface with small particles. However, from the IR spectra of adsorbed CO a definite impact of MnO on the chemisorptive properties of Rh is apparent (Fig. 4, Table 4). As discussed in the previous section, the effect of MnO on the IR spectra is not necessarily linked to the presence of MnO at the surface of the Rh particles. It is tentatively concluded here that MnO is present to a small extent only, if at all, at the Rh surface of very small particles. In Parts 2 and 3 (*10, 11*) we will provide additional evidence that the latter conclusion holds.

The reason for the contrast between the promoting effect of MnO with large and small particles might thus be related to the presence and absence, respectively, of MnO at the Rh surface. We propose that the absence of MnO at the metal surface is directly related to the size of the particles: for very small Rh particles one may envisage a rapid migration of MnO initially present at the surface of the particles to the metal–support interface. Here the MnO is strongly bound to the silica and is no longer effective for catalysis. For larger Rh particles the migration of MnO to the support might be impeded by (i) the larger distance between the metal surface and the support and (ii) the lower mobility of metal atoms for larger particles.

CONCLUSIONS

1. Silica-supported Rh catalysts with extremely high dispersion (H/Rh > 1) can be obtained by deposition–precipitation onto a

preformed carrier, using rhodium loadings between 2 and 6 wt%.

2. In Rh/MnO/SiO_2 catalysts prepared by deposition–precipitation the Rh and MnO phases are randomly distributed with respect to each other over the carrier. Infrared spectroscopy, however, reveals an influence of MnO on the interaction of CO with Rh.

3. A structure sensitivity of CO hydrogenation has been confirmed for Rh/SiO_2 since the product pattern shifts (to methanol) at high dispersions.

4. The enhancement of the activity of Rh-based catalysts for the hydrogenation of CO brought about by addition of MnO is apparent to a small extent only with highly dispersed catalysts. The absence of the promoting effect is probably due to the MnO not being present at the Rh surface.

ACKNOWLEDGMENTS

We are grateful to Ir. A. G. T. G. Kortbeek, Dr. F. G. A. van den Berg, and Dr. J. P. van den Berg for valuable discussions.

REFERENCES

1. Belgian Patent 824,822 to Union Carbide Corp. (1975).
2. Ellgen, P. C., Bartley, W. J., Bhasin, M. M., and Wilson, T. P., *Adv. Chem.* **178,** 147 (1979).
3. Ichikawa, M., *Bull. Chem. Soc. Japan* **51,** 2273 (1978).
4. van den Berg, F. G. A., Ph.D. thesis, Leiden, 1983.
5. Arakawa, H., Takeuchi, K., Matsuzaki, T. and Sugi, Y., *Chem. Lett.,* 1607 (1984).
6. Arakawa, H., Fukushima, T., Ichikawa, M., Takeuchi, K., Matsuzaki, T., and Sugi, Y., *Chem. Lett.,* 23 (1985).
7. Decanio, J., Onuferko, J. H., Foley, H. C., and Gates, B. C., *Surf. Sci.* **136,** L67 (1984).
8. Bosch, P., Acosta, D., Zenith, J., Nicolson, D. M., and Gates, B. C., *J. Mol. Catal.* **31,** 73 (1985).
9. Geus, J. W., *in* "Preparation of Catalysts, III" (G. Poncelet, P. Grange, and P. A. Jacobs, Eds.), p. 1. Elsevier, Amsterdam, 1983.
10. Kuipers, H. P. C. E., de Jong, K. P., and Knoester, A., Part 2 of this series, in preparation.
11. van Leerdam, G. C., Grongersma, H. H., Kuipers, H. P. C. E., and de Jong, K. P. Part 3 of this series, in preparation.
12. van Grondelle, M. C., and Zeen, P. J., *Anal. Chim. Acta* **116,** 397 (1980).
13. Kip, B. J., Duivenvoorden, F. B. M., Koningsberger, D. C., and Prins, R., *J. Catal.* **105,** 26 (1987).
14. Primet, M., Védrine, J. C., and Naccache, C., *J. Mol. Catal.* **4,** 411 (1978).
15. Primet, M., *J. Chem. Soc. Faraday Trans. 1* **74,** 2570 (1978).
16. Cavanagh, R. R., and Yates, J. T., *J. Chem. Phys.* **74,** 4150 (1981).
17. Worley, S. D., Rice, C. A., Mattson, G. A., Curtis, C. W., Guin, J. A., and Tarrer, A. R., *J. Chem. Phys.* **76,** 20 (1982).
18. Mesters, C. M. A. M., private communication.
19. Wilson, T. P., Kasai, P. H., and Ellgen, P. C., *J. Catal.* **69,** 193 (1981).
20. Niwa, M., and Lunsford, J. H., *J. Catal.* **75,** 302 (1982).
21. van Hardeveld, R., and Montfoort, A., *Surf. Sci.* **4,** 396 (1966).
22. Katzer, J. R., Sleight, A. W., Gajardo, P., Michel, J. B., Glaeson, E. F., and McMillan, S., *Faraday Discuss. Chem. Soc.* **72,** 121 (1981).
23. van 't Blik, H. F. J., van Zon, J. B. A. D., Huizinga, T., Vis, J. C., Koningsberger, D. C., and Prins, R., *J. Phys. Chem.* **87,** 2264 (1983).
24. Huizinga, T., Ph.D. thesis, Eindhoven, 1983.
25. Zaikovskii, V. I., Chalganov, E. M., Kuznetsov, B. N., Phyasova, L. M., and Yermakov, Yu.I., *React. Kinet. Catal. Lett.* **16,** 43 (1981).
26. Coenen, J. W. E., and Linsen, B. G., *in* "Physical and Chemical Aspects of Adsorbents and Catalysts" (B. G. Linsen, Ed.), p. 471. Academic Press, London, 1970.
27. de Jong, K. P., Geus, J. W., and Joziasse, J., *Appl. Surf. Sci.* **6,** 273 (1980).
28. Sata, H., and Shinozaki, S., *Surf. Sci.* **22,** 229 (1970).
29. Baker, R. T. K., *J. Catal.* **63,** 523 (1980).
30. Sachtler, W. M. H., *in* "Proceedings, 8th International Congress on Catalysis, Berlin, 1984," Vol. I, p. 151. Verlag-Chemie, Weinheim, 1984.